Transverse linearization for an underactuated compass-like biped robot and analysis of the closed-loop system

Leonid B. Freidovich and Anton S. Shiriaev

***Abstract*— We consider an impulsive 2-DOF mechanical system modeling dynamics of a planar two-link walker commonly known as a compass-gait biped. It is assumed that there is actuation in the hip but that the desired periodic trajectory describes an unstable passive walking gait. We recall and apply a recently developed technique for design of orbitally stabilizing feedback controllers. After that, we illustrate on the particular example how to assess various properties of the closed-loop system. In particular, sensitivity to perturbations of the slope of the walking surface is analyzed and possible deviations from the nominal trajectory are estimated analytically.**

***Index Terms*— Walking Robots; Underactuated Mechanical Systems; Periodic solutions; Orbital stabilization; Transverse Linearization; Virtual Holonomic Constraints**

I. INTRODUCTION

The study of simple walking devices is a fascinating field that has attracted considerable attention of researchers in the robotics and control communities. After McGeer's seminal paper [25], published in 1990, there was a series of publications, see e.g. [10], [11], [21], [18], [37], [5], [22], proposing and reporting how to find and analyze passive gaits for various low-dimensional walking devices.

These gaits are also of interest to consider in the case when some actuation is available since the corresponding desired trajectory is obviously efficient from the point of view of required nominal control efforts. The goal of the control design then is to stabilize an appropriate open-loop unstable limit cycle or to enlarge the regions of attraction that is typically very small when control is absent. We illustrate below how it can be done using a recently developed technique on a standard benchmark example: a planar two-link walker commonly known as a compass-gait biped.

The key idea of the approach is exploring a special but generic change of coordinates that can always be used for a parameterization of any nontrivial hybrid periodic solution of the walker dynamics. In essence, we avoid looking for explicit dependence on time but instead search for geometric relations among the time evolutions of the generalized coordinates [1], [12], [13] that should be valid along a cycle. Such relations are called *virtual holonomic constraints* [34], [40] and are rapidly becoming more and more broadly used for periodic motion planning and orbital feedback stabilization for mechanical systems with and without impacts, see e.g. [33], [40] and references therein. Knowledge of these relations allows introducing a moving Poincaré section [39], [14], [23], computing the Poincaré first-return map [29], [26], [20], as well as analytically deriving equations for a transverse linearization [16], [3], [36], [27], [31], [32].

We must remark that finding stable gaits for the compass-gait system has attracted many researchers motivated by various aspects of passive and active dynamic walking, see e.g. [8], [17], [15], [9], [19], [30], [2], [40], [24], [28] and references therein. However, to the best of our knowledge, there are no reported successful supplements for the other proposed stabilization or stability-verification techniques that allow systematic analytical or semi-analytical assessments of sensitivity to various perturbations and uncertainties. Below we provide an illustration of such analysis based on the approach using virtual holonomic constraints and analytical computation of transverse linearization. More precisely, we go one step further showing how to compute various characteristics of a periodic gait such as the rate of convergence, an estimate of the region of attraction, and sensitivity with respect to parameters exploiting some analytical (and therefore dimension independent) arguments.

L. Freidovich is with the Department of Applied Physics and Electronics, Umeå University, SE-901 87 Umeå, Sweden. A. Shiriaev is with the Department of Engineering Cybernetics, Norwegian University of Science and Technology, NO-7491 Trondheim, Norway and the Department of Applied Physics and Electronics, Umeå University, SE-901 87 Umeå, Sweden.

This work has been partly supported by the Swedish Research Council (grant 2008-5243), Kempe foundation, Young Researcher Award (Karriärbidrag) from Umeå University, and Russian Federal Agency for Science and Innovation (grant 02.740.11.5056).

II. DYNAMICS

Dynamics of a two-link compass-gait biped robot with a control torque u applied at the hip, schematically shown in Fig. 1, can be described by the impulsive system [11], [18], [38]

$$
\begin{cases}
\dot{x}_1 = x_2, \quad p_1\dot{x}_2 - p_2\cos(x_1-x_3)\dot{x}_4 - p_2\sin(x_1-x_3)x_4^2 \\
\qquad\qquad - p_4\sin x_1 = u \\
\dot{x}_3 = x_4, \quad p_3\dot{x}_4 - p_2\cos(x_1-x_3)\dot{x}_2 + p_2\sin(x_1-x_3)x_2^2 \\
\qquad\qquad + p_5\sin x_3 = -u \\
\text{as long as} \quad \cos(x_1+\psi) - \cos(x_3+\psi) \neq 0
\end{cases}
$$

$$
\begin{cases}
x_1^+ = x_3^-, \qquad x_3^+ = x_1^-, \qquad c^- = \cos(x_1^- - x_3^-), \\
\begin{bmatrix} x_2^+ \\ x_4^+ \end{bmatrix} = \begin{bmatrix} p_1 - p_2c^- & p_3 - p_2c^- \\ -p_2c^- & p_3 \end{bmatrix}^{-1} \\
\qquad\qquad \times \begin{bmatrix} p_7c^- - p_6 & -p_6 \\ -p_6 & 0 \end{bmatrix} \begin{bmatrix} x_2^- \\ x_4^- \end{bmatrix} \\
\text{whenever} \quad \cos(x_1^- + \psi) - \cos(x_3^- + \psi) = 0
\end{cases}
\tag{1}
$$

Preprint submitted to 8th IFAC Symposium on Nonlinear Control Systems.
Received January 21, 2010.

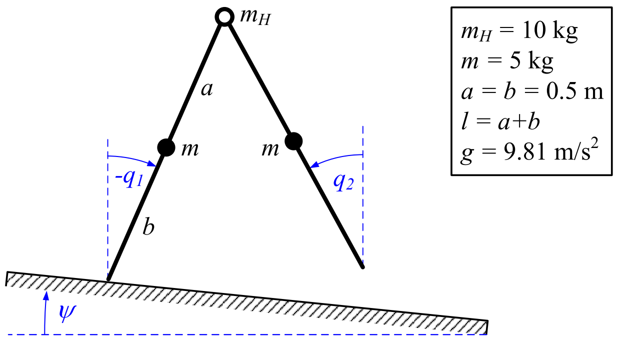

Fig. 1. Schematic of the compass-gait biped on a shallow slope ψ. Here, $q_1 = x_1$ and $q_2 = x_3$ describe the absolute angular positions of the stance leg and of the swing leg respectively. On the right, physical parameters of the compass-gait robot are listed.

Here the coefficients are defined by the physical parameters of the robot as follows:

$$p_1 = (m_H + m)l^2 + ma^2, \quad p_2 = mlb, \quad p_3 = mb^2,$$
$$p_4 = (m_H l + mb + ml)g, \qquad p_5 = mbg,$$
$$p_6 = mab, \qquad p_7 = m_H l^2 + 2mal,$$

the constant ψ denotes the slope of the walking surface and the standard abbreviations

$$x^- = x(t-) = \lim_{\varepsilon\to 0} x(t-|\varepsilon|), \quad x^+ = x(t+) = \lim_{\varepsilon\to 0} x(t+|\varepsilon|)$$

are used for the values before and after the jumps.

III. Description of a nominal periodic solution

A. Definition of a periodic solution

The dynamical system (1) can in short be rewritten as

$$\begin{aligned} \dot{x}(t) = f\big(x(t), u\big) \quad &\text{for} \quad x^- \notin \Gamma_-^\psi, \\ \Gamma_+^\psi \ni x^+ = F\big(x^-\big) \quad &\text{for} \quad x^- \in \Gamma_-^\psi \end{aligned} \tag{2}$$

with the state vector $x = [x_1,\ x_2,\ x_3,\ x_4]^T$, the surface Γ_-^ψ defined by $\cos\big(x_1^- + \psi\big) - \cos\big(x_3^- + \psi\big) = 0$, and $f(\cdot)$ and $F(\cdot)$ computed from the right-hand sides of the differential and algebraic equations respectively.

If there exist a number $T > 0$, a continuous scalar function $u = u_\star(t)$, and a continuous vector-function $x = x_\star(t)$ defined for $0 \le t \le T$ such that:

1) $x_\star(0) \in \Gamma_+^{\psi_0}$,
2) For $0 < t < T$: $x = x_\star(t)$ is continuously differentiable, does not cross[1] $\Gamma_-^{\psi_0}$, and satisfies the differential equation $\dot{x}_\star(t) = f\big(x_\star(t), u_\star(t)\big)$,
3) $x_\star(T) \in \Gamma_-^{\psi_0}$ and $F\big(x_\star(T)\big) = x_\star(0)$,

then, the solution $x_\star(t)$ is referred to as a *nominal periodic solution* of the hybrid system (2) describing dynamics of a compass-gait walking on a surface with the slope $\psi = \psi_0$.

[1]Crossings that are not heel strike related will be ignored here avoiding scuffing and impossibility for walking with fixed lengths of legs without knees and without passing through the surface.

B. Example of a periodic solution

For instance, if $\psi_0 = 2.87\,\pi/180$ and $u_\star(t) \equiv 0$, then there are two nontrivial periodic solutions [6]—passive gaits of the walker (1). One of them is defined by the following initial conditions:

$$\begin{aligned} x_{1\star}(0) &\approx 0.203177786690625, \\ x_{2\star}(0) &\approx -1.196561416996205, \\ x_{3\star}(0) &\approx -0.303359681764206, \\ x_{4\star}(0) &\approx -0.720513934734346. \end{aligned} \tag{3}$$

It is possible to verify that the initial conditions (3) with $u = u_\star(t) \equiv 0$ define an unstable periodic solution $x = x_\star(t) = x_\star(t+T)$ of the walker dynamics (1) with the period $T \approx 0.583723$ [sec].

This periodic solution, as well as any other one, can be also described differently.

C. Geometric description of a periodic solution

Suppose that for the nominal periodic solution $x = x_\star(t)$, such as the one with the initial conditions at (3), the component $x_{1\star}(t)$ is monotone on $0 \le t \le T$. Then, there exists a twice continuously differentiable function $\varphi(\theta)$, describing the synchronization between the joint angles along the periodic trajectory, such that

$$x_{1\star}(t) = \theta_\star(t), \qquad x_{3\star}(t) = \varphi\big(\theta_\star(t)\big). \tag{4}$$

Furthermore, the function $\theta = \theta_\star(t)$ for $0 \le t \le T$ can be computed by solving the following second order differential equation [35]

$$\alpha(\theta)\,\ddot{\theta} + \beta(\theta)\,\dot{\theta}^2 + \gamma(\theta) = 0, \tag{5}$$

where the coefficients are defined by the physical parameters of the walker:

$$\begin{aligned} \alpha(\theta) &= -p_2\big(\varphi'(\theta) + 1\big)\cos\big(\theta - \varphi(\theta)\big) + p_3\varphi'(\theta) + p_1, \\ \beta(\theta) &= p_2\left(1 - \big(\varphi'(\theta)\big)^2\right)\sin\big(\theta - \varphi(\theta)\big) \\ &\qquad -\varphi''(\theta)\left(p_2\cos\big(\theta - \varphi(\theta)\big) - p_3\right), \\ \gamma(\theta) &= -p_4\sin(\theta) + p_5\sin\big(\varphi(\theta)\big) \end{aligned} \tag{6}$$

The function $\varphi(\theta)$ that defines synchronization between the position coordinates along the periodic solution is known as a *virtual holonomic constraint* [34], [40]. The equation (5) is obtained substituting relations defined by (4) into a linear combination of the two differential equations in (1) that is *independent on the control input* u. It is sometimes called *reduced dynamics* or dynamics projected onto the manifold defined by the virtual constraint: $x_3 \equiv \varphi(x_1)$.

If there exists a periodic trajectory for a particular function $\varphi(\theta)$, it gives rise to a family of possible control inputs consistent with it, that include the ones that make the constraint invariant, see e.g. [42].

D. Control law for a periodic solution

Having known a nontrivial periodic solution $x = x_\star(t)$ of (2), one can compute the corresponding control input $u = u_\star(t)$ and, visa verse, for a given initial condition $x_\star(0)$ and a control input $u_\star(t)$, the solution $x_\star(t)$ is uniquely determined by (2). However, if one is interested in defining the control input in the form of a state feedback

$$u = U(x)$$

that satisfies the interpolation condition

$$u_\star(t) = U(x)|_{x=x_\star(t)}\,, \tag{7}$$

then, there are many choices for the function $U(x)$. One of them can be found as follows: Given a function $\varphi(\theta)$ that describes the time-evolution synchronization (4) between the degrees of freedom along the solution, substitute the relations

$$\begin{array}{ccc} q_1 = \theta, & \dot q_1 = \dot\theta, & \ddot q_1 = \ddot\theta \\ q_2 = \varphi(\theta), & \dot q_2 = \varphi'(\theta)\,\dot\theta, & \ddot q_2 = \varphi''(\theta)\,\dot\theta^2 + \varphi'(\theta)\,\ddot\theta \end{array} \tag{8}$$

into the two differential equations in (1) and solve the obtained system with respect to $\ddot\theta$ and u, see also [42], [40]. Then, one obtains

$$\begin{aligned} u = {} & (p_2^2\cos^2\big(\theta-\varphi(\theta)\big)\varphi''(\theta)\dot\theta^2 + (p_2\dot\theta^2\varphi'(\theta)(\varphi'(\theta)+1) \\ & \times \sin\big(\theta-\varphi(\theta)\big) + p_4\sin(\theta) + (p_5\sin\big(\varphi(\theta)\big)\varphi'(\theta))) \\ & \times p_2\cos\big(\theta-\varphi(\theta)\big) - p_2\dot\theta^2(\varphi'(\theta)^3p_3 + p_1\sin\big(\theta-\varphi(\theta)\big) \\ & - p_3\varphi'(\theta)p_4\sin(\theta) - p_1((p_5\sin\big(\varphi(\theta)\big)) + p_3\varphi''(\theta)\dot\theta^2)) \\ & /(-p_2(\varphi'(\theta)+1)\cos\big(\theta-\varphi(\theta)\big) + (p_3\varphi'(\theta)) + p_1) \\ & \equiv U\big(\theta,\dot\theta\big) \end{aligned} \tag{9}$$

and defines the operator U.

Note that for a passive gait, such as the one with the initial conditions (3), the function $U\big(\theta_\star(t),\dot\theta_\star(t)\big)$ in (9) is identically equal to zero.

E. Hybrid zero-dynamics

The feedback control law $u = U(\theta,\dot\theta)$, defined by (9), makes the zero-dynamics manifold

$$\mathcal{Z} = \big\{[x_1,x_2,x_3,x_4] :\, x_3 = \varphi(x_1),\, x_4 = \varphi'(x_1)\,x_2\big\}$$

invariant along the solutions of the continuous-in-time part of the dynamics of the closed-loop system (2), (9). In addition, it can be shown that the restriction of the discrete mapping $F(\cdot)$ to the curve $\gamma_- = \Gamma_-^{\psi_0}\bigcap\mathcal{Z}$ maps it into $\gamma_+ = \Gamma_+^{\psi_0}\bigcap\mathcal{Z}$, i.e. the *hybrid zero-dynamics* [41]

$$\begin{aligned} & x(0) \in \Gamma_+^{\psi_0}\textstyle\bigcap\mathcal{Z}, \\ & \dot x(t) = f|_{\mathcal{Z}}\Big(x(t), U\big(x_1(t),x_2(t)\big)\Big) \quad \text{for} \quad x^- \notin \Gamma_-^{\psi_0}, \\ & \Gamma_+^{\psi_0} \ni x^+ = F|_{\Gamma_-^{\psi_0}\bigcap\mathcal{Z}}\big(x^-\big) \quad \text{for} \quad x^- \in \Gamma_-^{\psi_0} \end{aligned} \tag{10}$$

is well-defined. However, the hybrid zero-dynamics in the considered case is not stable, i.e., the defined above periodic solution of the closed-loop system (10) is unstable.

If the zero-dynamics (10) was stable, a simpler feedback control design procedure for (1) than the one to be described shortly would be applicable. As an example, we refer to the technique recently developed and successfully tested on several walking-robot examples [41], [4], [40]. The idea there is to design a finite-time convergent or high-gain control input that forces the trajectory to the zero-dynamics manifold. Obviously, this approach cannot work in the situation with unstable hybrid zero-dynamics that we do have for the periodic solution described above.

Below we review an alternative transverse-linearization-based design that does not even require such dynamics to be well-defined, see also [13]. It is worth keeping in mind that the family of the feedback controllers to be presented includes all the controllers that can be designed using the notion of hybrid zero-dynamics.

IV. Orbital stabilization of the nominal cycle using transverse linearization

A generic approach for orbital stabilization of a periodic solution is to design a control input that stabilizes dynamics transversal to the trajectory of the solution.

A. Transverse coordinates

To introduce the transverse dynamics, consider the change of coordinates:

$$\begin{aligned} \begin{pmatrix} x_1 \\ x_2 \\ x_3 \\ x_4 \end{pmatrix} & \longleftrightarrow \begin{pmatrix} \theta = x_1 \\ \dot\theta = x_2 \\ y = x_3 - \varphi(x_1) \\ \dot y = x_4 - \varphi'(x_1)\,x_2 \end{pmatrix} \\ & \longleftrightarrow \begin{pmatrix} s = \Psi(x_1) \\ I = I(x_1,x_2) \\ y = x_3 - \varphi(x_1) \\ \dot y = x_4 - \varphi'(x_1)\,x_2 \end{pmatrix} \end{aligned} \tag{11}$$

where $\Psi(x_1)$ is defined as an inverse function[2] for $x_{1\star}(t)$, that can be computed as a solution $\theta = \theta_\star(t)$ of (5), i.e.

$$\theta_\star(s) = x_1 \qquad \Leftrightarrow \qquad s = \Psi(x_1), \tag{12}$$

the scalar function $I\big(\theta(t),\dot\theta(t)\big)$ is the conserved quantity[3] [35] for the equation (5)

$$I = \dot\theta^2(t) + \frac{2\left(\int_{\theta_\star(0)}^{\theta(t)} \alpha(s)\,\gamma(s)\,ds\right) - \alpha^2\big(\theta_\star(0)\big)\,\dot\theta_\star^2(0)}{\alpha^2\big(\theta(t)\big)} \tag{13}$$

with the functions $\alpha(\cdot)$ and $\gamma(\cdot)$ defined by (6).

The new coordinates are instrumental for design of orbitally stabilizing feedback controllers.

With the following feedback transformation

$$u = U\big(\theta,\dot\theta\big) + u_\perp, \tag{14}$$

[2]Here the monotonicity of $x_{1\star}(t) = \theta_\star(t)$ is exploited.

[3]The general expression proposed in [35] is simplified here using the fact that in (6) $\beta(\theta)$ is proportional to $\alpha'(\theta)$.

Preprint submitted to 8th IFAC Symposium on Nonlinear Control Systems.
Received January 21, 2010.

where $U(\cdot)$ is defined by (9), the dynamics (1) written in the variables $\{\theta,\ \dot\theta,\ y,\ \dot y\}$, see (11), becomes

$$\begin{aligned}&\alpha(\theta)\,\ddot\theta+\beta(\theta)\,\dot\theta^2+\gamma(\theta)=g(\theta,\dot\theta,y,\dot y,u_\perp),\\&\ddot y=h(\theta,\dot\theta,y,\dot y,u_\perp)\end{aligned}\qquad(15)$$

Assuming that $u_\perp(\theta,\dot\theta,y,\dot y)$ for (1) with (14) and (9) is chosen so that

$$\begin{aligned}\{y\equiv x_3-\varphi(x_1)=0,\quad \dot y\equiv x_4-\varphi(x_1)\,x_2=0,\\ I(x_1,x_2)=0\}\quad\Longrightarrow\quad u_\perp=0\end{aligned}$$

it can be shown that

$$x_\perp=\begin{bmatrix}I\\ y\\ \dot y\end{bmatrix}=\begin{bmatrix}I(x_1,x_2)\\ x_3-\varphi(x_1)\\ x_4-\varphi'(x_1)\,x_2\end{bmatrix}\qquad(16)$$

is a vector of transverse coordinates, i.e. coordinates that define deviations from the nominal periodic trajectory, while the variable s introduced in (11) defines location along it. Keeping s fixed and varying $x_\perp$, we obtain a surface transverse (in fact, orthogonal) to the nominal trajectory. The whole family of these surfaces is called a *moving Poincaré section* [23], [32]. In fact, it is possible to prove [32] that $\|x_\perp\|$ is equivalent to the distance between a point and the periodic trajectory in the first approximation.

B. Transverse linearization

Linearization along the periodic trajectory for the dynamics of the transverse coordinates (16) is a linear control system, whose solutions are determined by the rule [7]:

1) On the intervals $(i-1)\,T\le\tau<i\,T$, $i=1,\,2,\,\dots$, the solution $\hat x_\perp=\hat x_\perp(\tau)$ is defined by the linear control system

$$\tfrac{d}{d\tau}\,\hat x_\perp=A\big(\tau-(i-1)\,T\big)\,\hat x_\perp+B\big(\tau-(i-1)\,T\big)\,\hat u_\perp\qquad(17)$$

2) At the end of each interval, i.e. at $\tau=i\,T$, $i=1,\,2,\,\dots$, the solution $\hat x_\perp(i\,T-)$ experiences an instantaneous update defined by a linear transform

$$\hat x_\perp(i\,T+)=L\,\hat x_\perp(i\,T-)\qquad(18)$$

If control variables $u_\perp$ and $\hat u_\perp$ for the systems (15) and (17) are chosen small enough and related as

$$u_\perp=\hat u_\perp+\text{“small higher-order terms with respect to the distance to the target orbit of } x_\star(\cdot)\text{”}$$

then solutions of the linear system (17)–(18) initiated at $\hat x_\perp(0)=[I(0),\,y(0),\,\dot y(0)]^T$ are such that the transverse coordinates satisfy an approximation

$$x_\perp(t)=\hat x_\perp(s)+\text{“small higher-order terms”},\quad s=\Psi\big(x_1(t)\big)$$

provided τ is sufficiently distant from the time moments $(i-1)\,T,\ i\in\mathbb{N}$.

C. Continuous-in-time part of the transverse linearization

The matrix-function $A(\tau)$ in (17) is defined as [33], [31]

$$A=\begin{bmatrix}\mu(\tau)\,\big(g_I(\tau)-\beta(\theta_\star(\tau))\big) & \mu(\tau)\,g_y(\tau) & \mu(\tau)\,g_{\dot y}(\tau)\\ 0 & 0 & 1\\ h_I(\tau) & h_y(\tau) & h_{\dot y}(\tau)\end{bmatrix}\qquad(19)$$

where $\mu(\tau)=2\,\dot\theta_\star(\tau)/\alpha\big(\theta_\star(\tau)\big)$.

Here the functions $g(\cdot)$ and $h(\cdot)$ are taken from (15), subindices y and $\dot y$ denote the partial derivative with respect to y and $\dot y$, respectively, evaluated along the desired trajectory, and subindex I denotes the following directional derivative for $h(\cdot)$

$$h_I(\tau)=\left.\frac{\left(-\dfrac{\partial h(\theta,\dot\theta,0,0)}{\partial\theta}\,\ddot\theta+\dfrac{\partial h(\theta,\dot\theta,0,0)}{\partial\dot\theta}\,\dot\theta\right)}{2\,\left(\dot\theta^2+\ddot\theta^2\right)}\right|_{\theta\equiv\theta_\star(\tau)}\qquad(20)$$

with an analogous expression for $g_I(\cdot)$. It can be shown that our transformation (14) and (9) with $\varphi(\cdot)$ defined by a passive gait implies[4] $h_I(\cdot)\equiv 0$ and $g_I(\cdot)\equiv 0$. The matrix-function B in (17) is defined as follows

$$B(\tau)=\begin{bmatrix}\dfrac{2\,\dot\theta_\star(\tau)\,g_{u_\perp}(\tau)}{\alpha\big(\theta_\star(t)\big)} & 0 & h_{u_\perp}(\tau)\end{bmatrix}\qquad(21)$$

where $g_{u_\perp}$ and $h_{u_\perp}$ denote the partial derivatives with respect to $u_\perp$ evaluated along the desired trajectory.

D. Linearization of the update law

The update law in (18) is defined from the Jacobian of the nonlinear update law dF computed at $x_\star(T)$ as [7]

$$L=P^+_{n(0)}\,(dF)_{(x_\star(T))}\,P^-_{n(T)},\qquad(22)$$

with two matrices

$$P^-_{n(T)}=\left(I_4-\frac{n(T)\,\vec m_-^T}{n^T(T)\,\vec m_-}\right)\left(\begin{bmatrix}P(T)\\ n^T(T)\end{bmatrix}^{-1}\begin{bmatrix}I_3\\ 0_{1\times 3}\end{bmatrix}\right),$$

$$P^+_{n(0)}=P(0)\left(I_4-\frac{n(0)\,n^T(0)}{n^T(0)\,n(0)}\right)$$

combining appropriate orthogonal projections along $n(T)$ and $n(0)$ and linearization of the change of coordinates (11), defined by the following block of the Jacobian matrix

$$P(t)=\begin{bmatrix}-2\,\ddot\theta_\star(t) & 2\,\dot\theta_\star(t) & 0 & 0\\ -\varphi'(\theta_\star(t)) & 0 & 1 & 0\\ -\varphi''(\theta_\star(t))\,\dot\theta_\star(t) & -\varphi'(\theta_\star(t)) & 0 & 1\end{bmatrix}\qquad(23)$$

with $n(t)$ denoting the flow along the nominal trajectory

$$n(t)=\begin{bmatrix}\dot x_{1\star}(t)\\ \dot x_{2\star}(t)\\ \dot x_{3\star}(t)\\ \dot x_{4\star}(t)\end{bmatrix}=\begin{bmatrix}\dot\theta_\star(t)\\ \ddot\theta_\star(t)\\ \varphi'(\theta_\star(t))\,\dot\theta_\star(t)\\ \varphi''(\theta_\star(t))\,\dot\theta_\star^2(t)+\varphi'(\theta_\star(t))\,\ddot\theta_\star(t)\end{bmatrix},\qquad(24)$$

[4]These functions are not trivial with a possible alternative choice of (14) and $U(x_1,x_2)\equiv 0$ for a target passive gait.

and $\vec{m}_-$ being the normal vectors to $\Gamma_-^{\psi_0}$:

$$\vec{m}_- = \big[\sin\big(x_{1\star}(T)+\psi_0\big),\ -\sin\big(x_{1\star}(T)+\psi_0\big),\ 0,\ 0\big]^T \tag{25}$$

respectively. We skip the index ψ_0 here since it is easy to see that the operator L does not depend on the angle ψ.

E. Orbital stabilization

An orbitally stabilizing feedback control law for the nonlinear system (1), (14), (9) can be design based on successful stabilization of transverse linearization (17)–(18) as follows:

- Design a stabilizing controller

  $$\hat{u}_\perp = K\big(\tau-(i-1)\,T\big)\,\hat{x}_\perp \qquad \text{for} \quad (i-1)\,T \le \tau < i\,T$$

  for the linearization (17)–(18).
- Take

  $$u_\perp = K(s)\ x_\perp(t), \qquad s = \Psi\big(x_1(t)\big) \tag{26}$$

  with $x_\perp$ from (16).

In fact, orbital exponential stability of the nominal periodic solution for the closed-loop system follows from exponential stability of the linearization[5] [31].

Evolution of the states of (17)–(18) over the period is given by solutions of the discrete-time system

$$\hat{x}_\perp^{k+1} = L\,\Phi_K(T)\,\hat{x}_\perp^{k}. \tag{27}$$

Hence, the stability is ensured whenever the eigenvalues of the transition matrix $L\,\Phi_K(T)$ are strictly inside the unite circle. Here the matrix $\Phi(T)$ is computed solving the initial value problem

$$\tfrac{d}{d\tau}\,\Phi_K = \Big(A(\tau)+B(\tau)\,K(\tau)\Big)\Phi_K, \quad \Phi_K(0) = I_{3\times 3} \tag{28}$$

To design a stabilizing feedback control law for (17)–(18), for instance, one may search for the constant feedback gain taking a few steps towards solving the auxiliary optimization problem [7]

$$K(\tau) \equiv K_{opt} = \arg \min_{K(\tau)=\text{const}} \Big|\mathrm{eig}\Big\{L\,\Phi_K(T)\Big\}\Big|.$$

For the target trajectory defined by the passive hybrid cycle with the initial conditions (3), the gain

$$K_o = [-2,\ 14,\ 7] \tag{29}$$

ensures

$$\max\Big|\mathrm{eig}\Big\{L\,\Phi_K(T)\Big\}\Big|_{K=K_o} \approx 0.459254$$

indicating stability with the corresponding worst-case-scenario contraction rate. Note that having found $K(\tau)$ constant allows us to define the control law (14), (9), (26) without computing the function $\Psi(x_1)$ from (12).

[5]The new feature here with respect to the result of [31] is a constructive choice of the function $\Psi(\theta)$ instead of taking it as a generic identifier of the appropriate surface of the Poincaré section.

F. Region of attraction

It is important to realize that the discrete-time approximation system (27) can be used for a numerical-optimization based feedback control design but is useless for obtaining an approximation for the region of attraction for the nonlinear closed-loop system.

Here the computed linearization (17)–(18) might be useful. Let us sketch a possible approach to estimate a tube around the periodic trajectory where the solutions are trapped:

(1) Choose a matrix-function $Q(\tau) > \delta\,I_{3\times 3}$ and solve the matrix differential Lyapunov inequality

$$\tfrac{d}{d\tau}\,P(\tau) + A_{cl}^T(\tau)\,P(\tau) + P(\tau)\,A_{cl}(\tau) \le -Q(\tau)$$

for $0 \le \tau \le T$, where

$$A_{cl}(\tau) = A(\tau) + B(\tau)\,K(\tau) \tag{30}$$

such that $P(\tau) = P^T(\tau) > 0$ and the next strict inclusion of sets is valid

$$\Big\{\zeta_T : \big(L^{-1}\zeta_T\big)^T P(T)\big(L^{-1}\zeta_T\big) \le 1\Big\} \subset \Big\{\zeta_0 : \zeta_0^T P(0)\zeta_0 \le 1\Big\}$$

(2) Use the quadratic Lyapunov function candidate

$$V(t) = x_\perp^T(t)\,P(s)\,x_\perp(t), \qquad s = \Psi\big(x_1(t)\big)$$

with $x_\perp$ defined in (16), to obtain an estimate for the tube in the following form

$$\Omega = \big\{x :\ x_1 = \theta_\star(\tau),\ x_\perp^T(\tau)P(\tau)x_\perp(\tau) \le \varepsilon^2,\ 0 \le \tau < T\big\}$$

with some $\varepsilon > 0$. Note that the derivative of the Lyapunov function can be computed analytically and, since it is based on the linearization, it is negative for sufficiently small ε^2.

The conservativeness of this approach is currently under study. It is of interest to notice that the thinest places on this tube should indicate the possibly most sensible to perturbations locations along the periodic trajectory.

V. Sensitivity to perturbations of the slope

In the case when the slope of the walking surface ψ has its nominal value ψ_0, the nominal open-loop unstable periodic trajectory—the passive walking cycle of (1) with the initial conditions at (3)—becomes an exponentially orbitally stable solution of the closed-loop system (1), (14), (9), (26), (29).

However, if $\psi \ne \psi_0$, then the nominal periodic trajectory is not a solution of the closed-loop system, and the deviation from it is not characterized by solutions of the linear system (17)–(18). Below we suggest an appropriate modification for the transverse linearization (17)–(18) that can be used for approximating solutions of perturbed walker dynamics and that allows us to predict whether the trajectories stay in a tube around the nominal solution despite the slightly perturbed slope. Although we only consider sensitivity with respect to only one particular physical parameter, the procedure is straightforward to generalize.

Preprint submitted to 8th IFAC Symposium on Nonlinear Control Systems.
Received January 21, 2010.

A. Classification of perturbations

Suppose that the true slope $\psi(t)$ satisfies the inequality

$$|\psi(t) - \psi_0| \le |\bar{h}| \qquad \text{with} \qquad |\bar{h}| \quad \text{being sufficiently small}$$

and such that a solution exists and moreover, it has jumps due to impact at $t = \{T_k\}_{k\ge 1}$. The value of $\psi(t)$ is important only at the time moments $t = T_k$, $k \ge 1$; so, the following notation is useful

$$\psi(T_k) = \psi_0 + h_k \quad \text{with} \quad \max_k |h_k| \le |\bar{h}|.$$

The following cases of perturbations are of interest:

- impulse: $h_1 = \bar{h}$, $h_2 = h_3 = \cdots = 0$
- step: $h_k = \bar{h}$ $\forall k$,
- cyclic: $h_k = h_{k+N}$ $\forall k$, $N \ge 2$,
- stochastic: $\{h_k\}_{k\ge 1}$ is a stochastic process.

In the following, for simplicity, we will concentrate on the step perturbation.

B. Perturbed transverse dynamics

Whenever the switching surfaces are shifted by perturbations, i.e.

$$\Gamma_{\pm}^{\psi_0} \ne \Gamma_{\pm}^{\psi_0 + h_k}$$

the nominal transverse linearization (17)–(18) is of no use.

So, for a given sequence of perturbations $\{h_k\}$ to the slope ψ_0, let us introduce the following hybrid system[6]

1) On the intervals $(k-1)T - \delta_i^{k-1} \le \tau < kT + \delta_f^k$, $k = 1, 2, \ldots$, the solution $\hat{x}_\perp = \hat{x}_\perp(\tau)$ is defined by the linear control system
$$\tfrac{d}{d\tau}\, \hat{x}_\perp = A\big(\tau - (k-1)\,T\big)\, \hat{x}_\perp + B\big(\tau - (k-1)\,T\big)\, \hat{u}_\perp \tag{31}$$
2) At the end of each interval, i.e. at $\tau = kT + \delta_f^k$, $k = 1, 2, \ldots$, there is an instantaneous update

$$\hat{x}_\perp(kT + \delta_f^k) = \big[L + \triangle L_0(h_k)\big]\, \hat{x}_\perp(kT + \delta_f^k -) + \triangle L_1(h_k) \tag{32}$$

Here δ_i^{k-1} and δ_f^k are time distances needed for a trajectory to travel between $\Gamma_-^{\psi_0}$ and $\Gamma_-^{\psi_0 + h_{k-1}}$ and between $\Gamma_+^{\psi_0}$ and $\Gamma_+^{\psi_0 + h_k}$ respectively, while the changes in the linearization for the update law are due to the fact that the jump due to update happens at a value shifted from the nominal one.

Since the impact condition from (1)

$$\cos\big(x_1^- + \psi_0 + h_k\big) - \cos\big(x_3^- + \psi_0 + h_k\big) = 0$$

can be (locally) rewritten as $x_1^- + x_3^- + = -2\,(\psi_0 + h_k)$ and using the linear approximations

$$x_\star(T + \delta_f^k) = x_\star(T) + n(T)\, \delta_f^k + O\left((\delta_f^k)^2\right),$$
$$x_\star(-\delta_i^{k-1}) = x_\star(0) - n(0)\, \delta_i^{k-1} + O\left((\delta_i^{k-1})^2\right),$$

with $n(t)$ given in (25), it is not hard to see that

$$\delta_i^{k-1} \approx \frac{2\, h_{k-1}}{\dot\theta_\star(0)\Big(1 + \varphi'\big(\theta_\star(0)\big)\Big)}, \qquad \delta_f^k \approx \frac{-2\, h_k}{\dot\theta_\star(T)\Big(1 + \varphi'\big(\theta_\star(T)\big)\Big)} \tag{33}$$

up to small higher-order terms.

Now, we have

$$\begin{aligned}\triangle L_0(h_k) &= P^+_{n(-\delta_i^{k-1})}\, (dF)_{(x_\star(T+\delta_f^k))}\, P^-_{n(T+\delta_f^k)} \\ &\quad - P^+_{n(0)}\, (dF)_{(x_\star(T))}\, P^-_{n(T)}, \\ \triangle L_1(h_k) &= P^+_{n(-\delta_i^{k-1})}\, \Big(F\big(x_\star(T + \delta_f^k)\big) - x_\star(-\delta_i^{k-1})\Big)\end{aligned} \tag{34}$$

Therefore, the discrete-time system (27) transforms into

$$\hat{x}_\perp^{k+1} = A_k\, \hat{x}_\perp^k + \triangle L_1(h_k), \tag{35}$$

with

$$\begin{aligned} A_k = {} & (L + \triangle L_0(h_k))\, \Big(I_{3\times 3} + \delta_f^k\, A_{cl}(T)\Big)\, \Phi(T) \\ & \times \big(I_{3\times 3} - \delta_i^{k-1}\, A_{cl}(0)\big) + O\left((\delta_f^k)^2 + (\delta_i^{k-1})^2\right),\end{aligned}$$

where A_{cl} is from (30), Φ is defined by (28), L is from (25), the matrices A and B are defined in (19) and (21).

The obtained system allows quantifying response to possible perturbations in the slope for various scenarios. Let us see what can be done in the case when the slope is constant but different from nominal.

C. Sensitivity to step perturbations

In the case of step perturbation, i.e. $h_k = \bar{h}$ for $k \ge 1$, the system (35) can be rewritten as[7]

$$\hat{x}_\perp^{k+1} = \big(L\, \Phi(T) + \bar{h}\, P_\star\big)\, \hat{x}_\perp^k + \bar{h}\, \hat{x}_\perp^\star + O(\bar{h}^2), \tag{36}$$

up to the small higher-order terms.

Clearly, for the trajectories to stay in a small tube around the nominal motion it is necessary to have $\bar{h}$ so small that the eigenvalues of the matrix $\big(L\,\Phi(T) + \bar{h}\, P_\star\big)$ are inside the unite circle. An estimate for a bound on $\bar{h}$ can be obtained using the Lyapunov function candidate $V_k = (\hat{x}_\perp^k)^T\, P\, \hat{x}_\perp^k$, where $P = P^T > 0$ being a solution for

$$\big(L\, \Phi_K(T)\big)^T P\, L\, \Phi_K(T) - P = -\delta\, I_{3\times 3}$$

Along the solutions of (36) one obtains

$$\begin{aligned} V_{k+1} - V_k = {} & -(\hat{x}_\perp^k)^T\, \big(\delta\, I_{3\times 3} - 2\, \bar{h}\, P_\star^T P\, L\, \Phi(T)\big)\, \hat{x}_\perp^k \\ & + 2\, \bar{h}\, (\hat{x}_\perp^\star)^T P\, L\, \Phi(T)\, \hat{x}_\perp^k + O(\bar{h}^2)\end{aligned}$$

and therefore we must have

$$|\bar{h}| < \frac{\delta}{2\, \|P_\star^T P\, L\, \Phi(T)\|}.$$

Moreover, an asymptotic steady-state value for $x_\perp(t)$ after each impact can be estimated from (36) as follows

$$x_\perp(kT+) \approx \hat{x}_\perp^k \to \bar{h}\, \big(I_{3\times 3} - L\, \Phi(T)\big)^{-1}\, \hat{x}_\perp^\star + O(\bar{h}^2) \tag{37}$$

[6]Of course, this system reduces to (17)–(18) if $\bar{h} = 0$. Note that we naturally assume that the definition of the solution for the continuous-in-time part of the dynamics can be extended to a slightly bigger interval whenever this is needed.

[7]In [19], it is suggested to compute an approximation for this system via numerical simulations assuming that $P_\star \approx 0$. It is not clear to us how to introduce sensitivity gains analogous to the ones proposed in [19] rigorously taking into account the fact that $P_\star \ne 0$.

as $k \to \infty$, where

$$\hat{x}_\perp^\star = -2P^+_{n(0)} \left(\frac{(dF)_{(x_\star(T))}\, n(T)}{\dot\theta_\star(T)\Big(1+\varphi'\big(\theta_\star(T)\big)\Big)} + \frac{n(0)}{\dot\theta_\star(0)\Big(1+\varphi'\big(\theta_\star(0)\big)\Big)} \right)$$

is defined only by the target trajectory and is independent on the choice of the control law.

For sufficiently small values of $\bar h$ existence of this estimate imply boundedness of $x_\perp(t)$, existence of the solutions of the closed-loop system initiated sufficiently close to $x_\star(0)$ on the infinite interval of time, and the fact that these solutions stay in a small tube around the nominal trajectory, radius of which is proportional to $\bar h$ in the first approximation.

Note that the estimate (37) tells us that having the eigenvalues of the matrix $L\,\Phi(T)$ too close to the boundary of the unite circle would result in an enormous sensitivity to perturbations from the nominal value of the slope. From the other hand, we can see that even if the controller is very aggressive, the possible deviations strongly depend on how the planned periodic trajectory crosses the impact surfaces.

A positive conclusion is that despite the fact that there is no guarantee that the obtained solutions are asymptotically periodic, the motions will be very similar to the nominal one provided perturbations of the slope are sufficiently small.

For our set of parameters, we have

$$\hat{x}_\perp^\star \approx [6.153393,\ \ -1.777320,\ 4.638892]^T,$$

which does not depend on the choice of the control law, and the steady-state error after impacts

$$\begin{aligned} \bar{x}_\perp &= \bar h \left(I_{3\times 3} - L\,\Phi(T)\right)^{-1} \hat{x}_\perp^\star + O(\bar h^2) \\ &\approx \bar h\ [9.462,\ \ -2.817,\ 12.984]^T + O(\bar h^2) \end{aligned}$$

for the particular choice $K = K_o$, while a direct search for the values of $\bar h$ making the matrix $\left(L\,\Phi(T) + \bar h\, P_\star\right)$ unstable results in the values outside the interval

$$-0.187 < \bar h < 0.388$$

and this estimate is clearly too rough since it is obtained dropping all the $O(\bar h^2)$ terms.

VI. Results of Numerical Simulations

The first useful thing to verify is how close the trajectories of (17)–(18) approximate the trajectories of (1), (9), (14), (26) taking in both cases $K(\cdot) \equiv K_o = [-2,\ 14,\ 7]$ and the nominal value of the slope $\psi = \psi_0$.

The result of simulation with initial conditions obtained by random perturbation from (3) are given in Fig. 2. Here we plot $x_\perp(t)$ and $\hat{x}_\perp(\tau)$ and the qualitative similarity is obvious; we observe the fact that the jumps are not simultaneous.

Computing s according to (12) and plotting $x_\perp(t)$ as a function of s allows to push the two systems into the same time scale. This is shown below in Fig. 3.

To verify the estimate for the steady-state error after impact, obtained from (36), we take $h_k = \bar h = 0.003$ and run the simulations with the same initial conditions expecting to observe convergence to $\bar{x}_\perp \approx [0.028,\ \ -0.0085,\ 0.039]^T$. The result confirming our expectations is shown in Fig. 4.

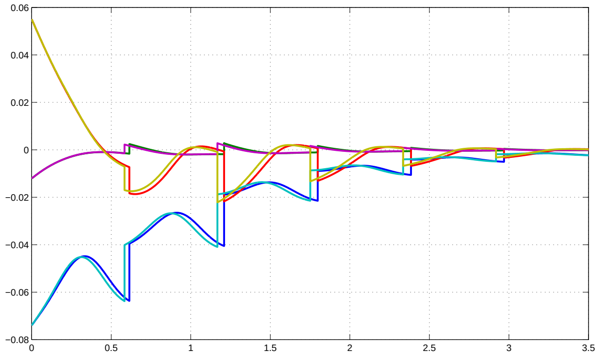

Fig. 2. The time evolution of the components of $x_\perp(t)$ and $\hat{x}_\perp(\tau)$ in the case of the nominal slope $\psi = \psi_0$.

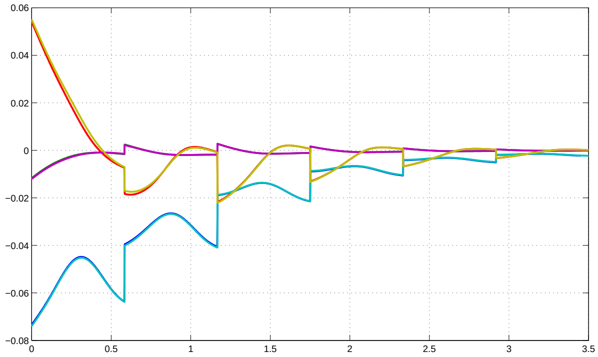

Fig. 3. The time evolution of the components of $x_\perp(t)$ versus $s = \Psi(x_1(t))$ and $\hat{x}_\perp(\tau)$ versus τ in the case of the nominal slope $\psi = \psi_0$.

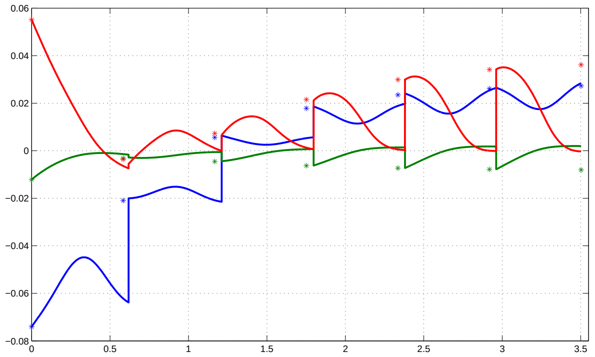

Fig. 4. The time evolution of the components of $x_\perp(t)$ in the case of the perturbed slope $\psi = \psi_0 + \bar h$ (solid) and the solution of the appropriately initiated discrete-time system (36) with dropped $O(\bar h^2)$ terms (dots).

VII. Conclusion

We have considered a 2-DOF impulsive mechanical system describing dynamics of the compass-gait biped walking robot with actuation at the hip. The system admits an open-loop-unstable periodic solution, which leads to unstable hybrid zero-dynamics. We apply a recently developed technique for orbital stabilization of impulsive mechanical systems with arbitrary number of passive gaits: an exponentially orbitally stabilizing feedback control law is designed using the notions

Preprint submitted to 8th IFAC Symposium on Nonlinear Control Systems.
Received January 21, 2010.

of virtual holonomic constraints and transverse linearization. The challenging nonlinear control problem is reduced to regulation of a linear impulsive system of reduced dimension. The latter is solved here through numerical optimization.

The contribution is showing how to analyze various properties of the closed-loop system. In particular, we have studied response of the system to step perturbations in the slope of the walking surface from the nominal value used at the control design stage. A new linear system that can be interpreted as a perturbation of the transverse linearization is obtained analytically. The computations are generalizable for analysis of sensitivity to various other parametric uncertainties and may be computationally tractable for higher dimensional models.

REFERENCES

[1] Y. Aoustin and A. Formal'sky, "Design of reference trajectory to stabilize desired nominal cyclic gait of a biped," in *Proc. of the Intern. Workshop on Robot Motion and Control*, Kiekrz, Poland, Jun. 1999, pp. 159–164.

[2] F. Asano and Z.-W. Luo, "Asymptotically stable gait generation for biped robot based on mechanical energy balance," in *Proc. of the 2007 IEEE/RSJ Intern. Conf. on Intelligent Robots and Systems*, San Diego, CA, USA, Nov. 2007, pp. 3327–3333.

[3] A. Banaszuk and J. Hauser, "Feedback linearization of transverse dynamics for periodic orbits," *Systems and Control Letters*, vol. 26, pp. 95–105, 1995.

[4] C. Chevallereau, G. Abba, Y. Aoustin, F. Plestan, E. Westervelt, C. Canudas-de-Wit, and J. Grizzle, "RABBIT: A testbed for advanced control theory," *IEEE Control Systems Magazine*, vol. 23, no. 5, pp. 57–79, 2003.

[5] S. Collins, A. Ruina, R. Tedrake, and M. Wisse, "Efficient bipedal robots based on passive dynamic walkers," *Science Magazine*, vol. 307, pp. 1082–1085, 2005.

[6] L. Freidovich, U. Mettin, A. Shiriaev, and M. Spong, "A passive 2-dof walker: Hunting for gaits using virtual holonomic constraints," *IEEE Trans. on Robotics*, vol. 25, no. 5, pp. 1202–1208, 2009.

[7] L. Freidovich, A. Shiriaev, and I. Manchester, "Stability analysis and control design for an underactuated walking robot via computation of a transverse linearization," in *Proc. of the 17th IFAC World Congress*, Seoul, Korea, Jul. 2008, pp. 10 166–10 171.

[8] M. Garcia, A. Chatterjee, A. Ruina, and M. Colenman, "The simplest walking model: stability, complexity, and scaling," *ASME Journal of Biomedical Engineering*, vol. 120, no. 2, pp. 281–288, 1998.

[9] D. Gates, J. Su, and J. Dingweil, "Possible biomedical origins of the long-range correlations in stride intervals of walking," *Physica A*, vol. 380, pp. 259–270, 2007.

[10] A. Goswami, B. Espiau, and A. Keramane, "Limit cycles in a passive compass gait biped and passivity-mimicking control laws," *Journal of Autonomous Robots*, vol. 4, no. 3, pp. 273–286, 1997.

[11] A. Goswami, B. Thuilot, and B. Espiau, "A study of the passive gait of a compass-like biped robot," *Intern. Journal of Robotics Research*, vol. 17, no. 12, pp. 1282–1301, 1998.

[12] J. Grizzle, G. Abba, and F. Plestan, "Proving asymptotic stability of a walking cycle for a five dof biped robot model," in Proc. of the 2nd Intern. Conf. on Climbing and Walking Robots, Portsmouth, UK, 1999, pp. 69–81.

[13] ——, "Asymptotically stable walking for biped robots: Analysis via systems with impulse effects," *IEEE Trans. on Automatic Control*, vol. 46, no. 1, pp. 51–64, 2001.

[14] J. Hale, *Ordinary Differential Equations*. Malabar: Krieger, 1980.

[15] J. Hass, J. Herrmann, and T. Geisel, "Optimal mass distirbution for passivity-based bipedal robots," *Intern. Journal of Robotics Research*, vol. 25, no. 11, pp. 1087–1098, 2006.

[16] J. Hauser and C. Chung, "Converse Lyapunov functions for exponentially stable periodic orbits," *Systems and Control Letters*, vol. 23, no. 1, pp. 27–34, 1994.

[17] K. Hirata and H. Kokame, "Stability analysis of linear systems with state jump—motivated by periodic motion control of passive walker," in *Proc. of the IEEE Conf. on Control Applications*, Istanbul, Turkey, Jun. 2003, pp. 1085–1992.

[18] I. Hiskens, "Stability of hybrid system limit cycles: Application to the compass gait biped robot," in *Proc. of the 40th IEEE Conf. on Decision and Control*, Orlando, USA, Dec. 2001, pp. 774–779.

[19] D. Hobbelen and M. Wisse, "A disturbance rejection measure for limit cycle walking: the gait sensitivity norm," *IEEE Trans. on Robotics*, vol. 23, no. 6, pp. 1213–1224, 2007.

[20] Y. Hurmuzlu, F. Genot, and B. Brogliato, "Modeling, stability and control of biped robots - a general framework," *Automatica*, vol. 40, no. 10, pp. 1647–1664, 2004.

[21] A. Kuo, "Stabilization of lateral motion in passive dynamic walking," *Intern. Journal of Robotics Research*, vol. 18, no. 9, pp. 917–930, 1999.

[22] ——, "Choosing your steps carefully: Trade-offs between economy and versatility in dynamic walking bipedal robots," *IEEE Robotics and Automation Magazine*, vol. 14, no. 2, pp. 18–29, 2007.

[23] G. Leonov, "Generalization of the Andronov-Vitt theorem," *Regular and chaotic dynamics*, vol. 11, no. 2, pp. 281–289, 2006.

[24] N. Liu, J. Li, and T. Wang, "Passive walking that can walk down steps: simulation and experiments," *Acta Mechanica Sinica*, vol. 24, pp. 569–573, 2008.

[25] T. McGeer, "Passive dynamic walking," *Intern. Journal of Robotics Research*, vol. 9, no. 2, pp. 62–82, 1990.

[26] S. Nersesov, V. Chellaboina, and W. Haddad, "A generalization of Poincaré's theorem to hybrid and impulsive dynamical systems," *Intern. Journal of Hybrid Systems*, vol. 2, no. 1, pp. 39–55, 2002.

[27] C. Nielsen and M. Maggiore, "On local transverse feedback linearization," *SIAM Journal on Control and Optimization*, vol. 7, no. 5, pp. 2227–2250, 2008.

[28] J. Norris, A. Marsh, K. Granata, and S. Ross, "Revisiting the stability of 2D passive biped walking: Local behavior," *Physica D*, vol. 237, no. 23, pp. 3038–3045, 2008.

[29] H. Poincaré, *Oeuvres comleés*. Paris, France: Gauthier-Villars, 1916-1954, vol. 11.

[30] A. Safa, M. Saadat, and M. Naraghi, "Passive dynamic of the simplest walking model: replacing ramps with stairs," *Mechanics and Machine Theory*, vol. 42, pp. 1314–1325, 2007.

[31] A. Shiriaev and L. Freidovich, "Transverse linearization for impulsive mechanical systems with one passive link," *IEEE Trans. on Automatic Control*, vol. 54, no. 12, pp. 2882–2888, 2009.

[32] A. Shiriaev, L. Freidovich, and S. Gusev, "Transverse linearization for controlled mechanical systems with several passive degrees of freedom," *IEEE Trans. on Automatic Control*, vol. 55, no. 4, 2010.

[33] A. Shiriaev, L. Freidovich, and I. Manchester, "Can we make a robot ballerina perform a pirouette? Orbital stabilization of periodic motions of underactuated mechanical systems," *Annual Reviews in Control*, vol. 32, no. 2, pp. 200–211, 2008.

[34] A. Shiriaev, J. Perram, and C. Canudas-de-Wit, "Constructive tool for orbital stabilization of underactuated nonlinear systems: Virtual constraints approach," *IEEE Trans. on Automatic Control*, vol. 50, no. 8, pp. 1164–1176, 2005.

[35] A. Shiriaev, J. Perram, A. Robertsson, and A. Sandberg, "Periodic motion planning for virtually constrained Euler–Lagrange systems," *Systems and Control Letters*, vol. 55, pp. 900–907, 2006.

[36] G. Song and M. Zefran, "Stabilization of hybrid periodic orbits with application to bipedal walking," in *Proc. of the 2006 American Control Conf.*, Minneapolis, USA, Jun. 2006, pp. 2504–2509.

[37] M. Spong and F. Bullo, "Controlled symmetries and passive walking," *IEEE Trans. on Automatic Control*, vol. 50, no. 7, pp. 1025–1031, 2005.

[38] M. Spong, J. Holm, and D. Lee, "Passivity-based control of bipedal locomotion," *IEEE Robotics and Automation Magazine*, vol. 14, no. 2, pp. 30–40, 2007.

[39] M. Urabe, *Nonlinear Autonomous Oscillations*. New York: Academic Press, 1967.

[40] E. Westervelt, J. Grizzle, C. Chevallereau, J. Choi, and B. Morris, *Feedback Control of Dynamic Bipedal Robot Locomotion*. CRC Press, Taylor and Francis Group, 2007.

[41] E. Westervelt, J. Grizzle, and D. Koditschek, "Hybrid zero dynamics of planar biped walkers," *IEEE Trans. on Automatic Control*, vol. 48, no. 1, pp. 42–56, 2003.

[42] E. Westervelt, B. Morris, and K. Farrell, "Sample-based hzd control for robustness and slope invariance of planar passive bipedal gaits." *Autonomous Robots*, vol. 23, pp. 131–145, 2007.

Preprint submitted to 8th IFAC Symposium on Nonlinear Control Systems.
Received January 21, 2010.